DOI: 10.4408/IJEGE.2013-06.B-15

PORE PRESSURE DISTRIBUTIONS IN BRITTLE TRANSLATIONAL ROCKSLIDES

Simon LOEW[(*)] & Thomas STRAUHAL[(**,***)]

[(*)]Engineering Geology - Sonnegstrasse 5, ETH Zurich, CH-8092 Zurich, Switzerland - E-mail: simon.loew@erdw.ethz.ch
[(**)]alpS - Centre for Climate Change Adaptation Technologies - Grabenweg 68 - A-6020 Innsbruck, Austria
[(***)]University of Innsbruck - Institute of Geology and Paleontology - Innrain 52 - A-6020 Innsbruck, Austria
E-mail: strauhal@alps-gmbh.com

ABSTRACT

In this paper, we systematically study steady-state pore pressure conditions in translational brittle rockslides, with special focus on saturated and unsaturated flow in variably fractured rock masses. The study includes a discussion of critical hydraulic borehole observations in translational rockslides from British Columbia, Norway and the Italian Alps and explains these observations with a generic numerical rockslide model. Most key observations, such as piezometric pore pressure levels at the base of translational rockslides, the location of seepage faces, pressure compartments, perched groundwater flows, and deep groundwater tables can be successfully explained. Open questions relate to the magnitudes of negative pore pressures in the unsaturated zones and the impacts of strong heterogeneity in hydraulic conductivity fields. The impacts of suction and seepage forces on slope stability are discussed.

Key words: *rockslide, pore pressure, groundwater, translational slide, fractured rock, suction, stability*

1 INTRODUCTION

In contrast to slopes in soils and weak rocks, only few investigations exist which focus on the analysis of pore pressure measurements in brittle rock-slopes composed of fractured crystalline rock. Based on the experiences made at Vajont, most of these borehole-based investigations have been carried out in rockslides adjacent to hydropower lakes such as the Downie Slide (Imrie *et alii,* 1991; Kalenchuk *et alii,* 2012), Dutchman's Ridge Slide (Moore & Imrie 1995), and Little Chief Slide (Watson *et alii,* 2007), located along the Columbia River in Canada. In addition, detailed hydrogeological investigations have been carried out in hazardous rock-slopes along populated fjords (Aknes Slide in western Norway; e.g. Groneng *et alii,* 2011), or along hydropower drifts and penstocks (Rosone Slide in Orco Valley, Italy; e.g. Pisani *et alii,* 2010).

Most of these rockslides can be approximated as planar slides with multiple sliding surfaces composed of cataclastic breccia or fine-grained gouge, either stretching over the entire valley slopes between river bottom and crest line, or only occurring in the lower slope sector (Fig. 1). The compartments between these active sliding planes show diverse kinematic behavior, ranging from extensional faulting to compressive thrusting and buckling. Fine-grained shear and damage zones composed of clay gouge typically act as boundaries for pore pressure compartments within which selected fractures form preferential groundwater pathways. Piezometric levels from isolated borehole sections are remarkably complex and document both deep as well as shallow and artesian pore pressures at the level of the major sliding surfaces (Fig. 1). In addition, some slides show the occurrence of deep unsaturated zones below perched aquifers bounded by near surface shear zones. Pore pressure transients are

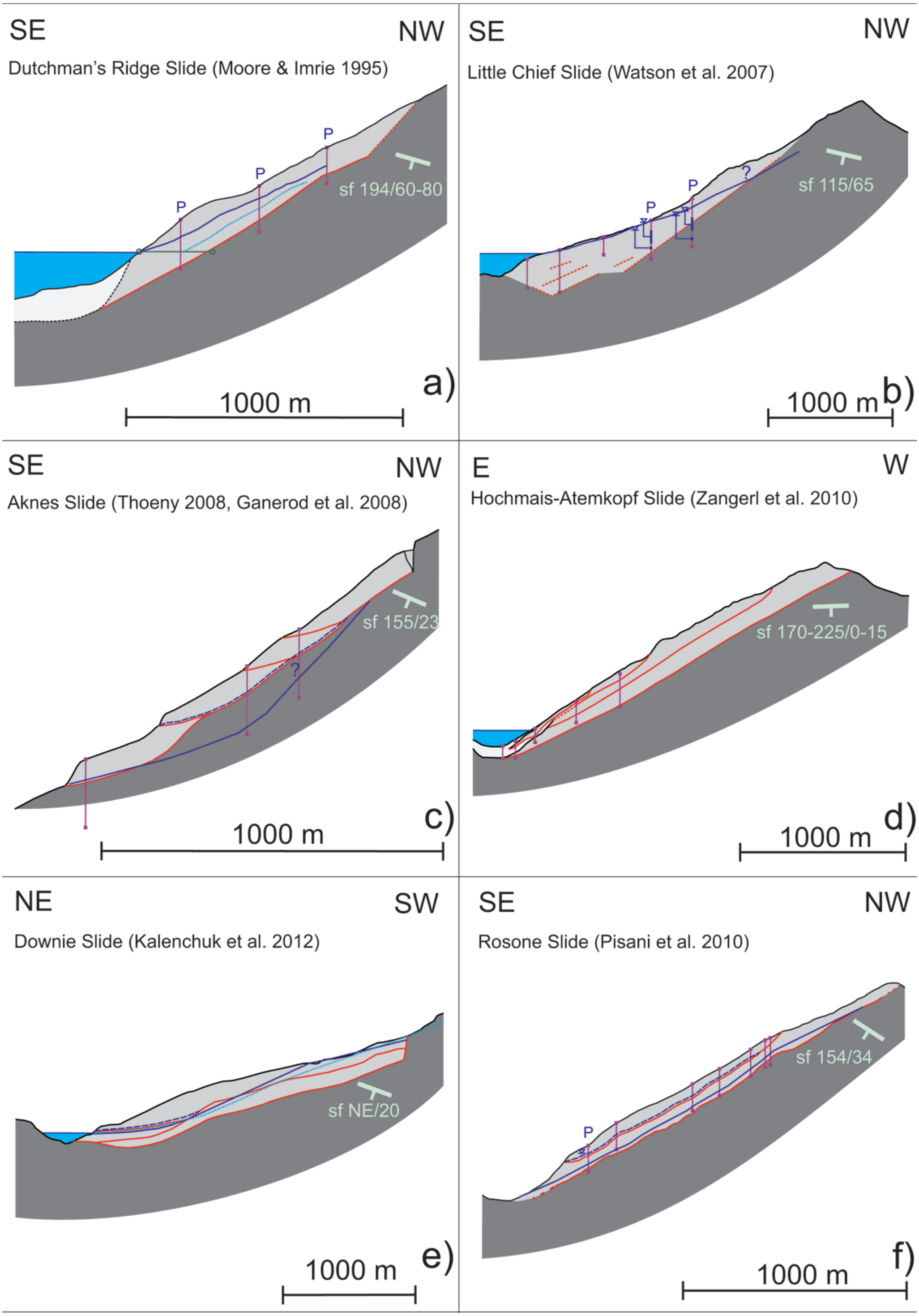

Fig. 1 - Translational rockslide geometry, foliation dip azimuth and angle, drainage gallery (green line), sliding planes (red lines), pressure monitoring boreholes and piezometric levels before drainage (blue lines): continuous line: lower phreatic groundwater table, dashed line: perched upper groundwater table, dotted line: confined pressure below basal sliding plane

controlled both by annual variation in recharge and lake level fluctuations. This paper reviews predisposition and critical hydraulic observations in these 5 crystalline rockslides (chapter 2), develops a generic hydrogeological model for translational rockslides with variably saturated fractured rock (chapter 3), numerically investigates the pore pressure distributions (including suction) and groundwater flows in the saturated, as well as unsaturated zones (chapter 4) and finally discusses the potential implications of variably saturated groundwater flow on translational rockslide stability (chapter 5). This study is not applicable for toppling slopes or strongly rotational/compound slides, where the internal deformation or slide geometry causes different types of permeability distributions. The focus of this study is mainly on brittle rockslides as they have a much higher probability for catastrophic failure than rockslides composed of weak rocks (e.g. Hungr *et alii,* 2005).

HYDRAULIC OBSERVATIONS IN CRYSTALLINE ROCKSLIDES

PREDISPOSITION

This paper only discusses quasi-planar slopes, which can be approximated with 2D flow and plane strain conditions in a vertical plane, striking normal to the mean slope orientation. However, some of these planar slopes and rockslides are laterally bounded by deep fluvial incisions, which might act as local receiving streams with out-of-plane directed flow lines and strains.

First, detailed borehole based hydraulic investigations of brittle rockslides were carried out in the late sixties for hydropower projects along the Columbia River in British Columbia - following the catastrophe of Vajont in 1963. First data sets from these Canadian projects were published in the early nineties (Imrie *et alii,* 1992, Moore & Imrie 1992, Moore 1992), describing multilevel piezometers installed in the Downie and Dutchman's Ridge Slide. Later, detailed hydraulic and mechanical subsurface investigations were reported from the nearby Little Chief Slide (Watson *et alii,* 2007) and Downie Slide (Kalenchuk *et alii,* 2012). These slides occur on the western side of the north-south oriented Columbia River, with the main foliation and bedding of the high-grade metamorphic rocks (granodiorites, gneisses and shists) dipping obliquely into the slope (Dutchman's Ridge, Little Chief) or parallel to the slope (Downie Slide). As shown on Figure 1 all these slides have a deep, basal sliding surface (200-250 m), a bulge at the toe, and override Quaternary deposits (glacial till, sand and gravel). Slope and sliding planes dip at Downie Slide with 18°, and at Little Chief and Dutchman's Ridge with 28° to 36°. The topography surrounding Dutchman's Ridge Slide is not planar, but controlled by two deep incisions, intersecting in the middle part of the slope (Figure 1), where the rockslide terminates as well. Downie and Dutchman's Ridge Slides were drained with 2400 and 800 m long drainage galleries located below or within the sliding mass from which large numbers of drainage holes (13'700 and 17'000 drilling meters) were drilled into the sliding rock mass.

At the Aknes slide in Western Norway and the Rosone Slide in the Italian Western Alps, hydraulic borehole investigations were restricted to fewer boreholes [6 at Aknes, 4 at Rosone], where pore pressures were primarily recorded in long open borehole intervals (Binet *et alii,* 2007; Groneng *et alii,* 2011). The rockslide at Aknes occurs in the lower sector of a slope dipping with 30-35° towards the fjord Storfjorden. Sliding occurs along foliation parallel cataclastic shear zones in granitic to dioritic orthogneisses daylighting along subordinate low-angle thrust surfaces at different elevations above the shoreline (Ganerod *et alii,* 2008). The western boundary of the translational slide is formed by a fluvial incision, which is of similar depth as the main sliding plane (at about 50 m depth). This leads to substantial drainage of the sliding mass towards this lateral incision, as supported by tracer tests with fluorescent dyes (Frei 2008). The Bertodasco sector of the Rosone rock-slope instability shows a typical slope inclination (31°) and sliding planes at 50 and 120 m depth with similar orientation (Pisani *et alii,* 2010). Sliding occurs along foliation parallel shear zones in Augengneiss. The morphology is complex, as the sliding zone terminates at a ridge separating the Orco and Piantonetto valleys. The Hochmais-Atemkopf rockslide in the Gepatsch Valley (Austria) has been studied intensively (Zangerl *et alii,* 2010) as it could potentially endanger the Gepatsch hydropower reservoir. Available data include structure, geomechanical and displacement data but not borehole based hydraulic measurements. The basal sliding surface dips with 31° (like the mean slope dip) and occurs at a maximum depth of 220 m. The currently active mass is constrained to the uppermost sliding plane - a 4 m thick shear zone - occurring at a depth of 30-50 m and dipping about 33°.

OBSERVED WATER TABLES AND PORE PRESSURE DISTRIBUTIONS

Prior to constructing drainage galleries, the subsurface hydraulic conditions at the Downie, Dutchman's Ridge and Little Chief Slides were investigated by exploratory adits and monitoring boreholes equipped with large numbers of multiple piezometers. These piezometers consisted of 1-2 m long monitoring sections isolated by Westbay multi-packer systems. In addition, pore pressure profiles were recorded during drilling using a single packer isolating the lowermost borehole section. As shown on Figure 1 piezometric pressures at the base of Downie Slide prior to drainage showed artesian conditions in the upper slope portion (500-700 m above Columbia River), shallow phreatic groundwater levels (up to 100 m below ground surface) in the mid-slope portion and seepage conditions in the lower-most slope section above the Columbia River. Such artesian pressures are in fact typical for rockslides containing massive layers of weak rocks, such as for example Campo-Vallemaggia (Bonzanigo *et alii,* 2007). The piezometric pressure levels within the Dutchman's Ridge Slide prior to drainage have been about 100 m below ground level for the upper and middle rockslide section, and at ground surface close to the Columbia River (Fig. 1). Deep piezometer intervals in the middle slope section show confined pore pressures below the basal sliding surface.

At Downie Slide pore pressure transients from drainage holes lead to observable pressure reactions over large distances (600 m) even across major clay rich shear zones, indicating the existence of higher conductive windows through these shear zones (Imrie *et alii,* 1991). This contrasts to Dutchman's Ridge and Little Chief Slides, which show strongly developed pressure compartments separated by persistent low permeability fault zones forming the basal sliding plane as well as steeply dipping pressure boundaries (Moore & Imrie 1995). In extreme cases, hydraulic head differentials of 50 and 75 m were observed across a 150 mm layer of clay gouge or a 1.5 m long packer. Consequently, drainage at Dutchman's Ridge Slide required a larger number and length of drain holes. Within pressure compartments of all three rockslides, large aperture fractures locally form highly conductive preferential groundwater pathways extending over distances of up to 600-700 m.

Water pressure measurements in Aknes and Rosone are mainly based on open hole piezometric levels in 100-200 m deep boreholes. In slopes showing significant vertical head gradients, such water table measurements represent complex mixtures of pressure heads, that cannot be resolved without detailed knowledge of the local permeability profiles. Water table measurements and optical image logging carried out during drilling operations at Aknes showed perched groundwater in the lower section of the highly fractured rockslide mass above the major sliding plane (at 50 m depth) and locally unsaturated conditions down to end of 200 m deep boreholes (Thoeny 2008). Similar conditions have been observed at Rosone (Binet *et alii,* 2007).

GENERIC TRANSLATIONAL ROCKSLIDE MODEL

ROCKSLIDE STRUCTURE AND GEOMETRY

A generic translational rockslide model was set up in the finite element code Geo-Slope Seep/W 2007 (GEO-SLOPE International Ltd 2008) to analyze saturated/unsaturated pore pressure variations in a translational rockslide with similar properties as the cases discussed above. The model represents translational rockslides with single or multiple planar sliding surfaces oriented parallel to a linear slope with a dip angle of 35° (Fig. 2). A basal sliding zone with a typical thickness of 5 m was defined 100 m below ground surface and is heading up to the crest. A secondary sliding plane with a thickness of 5 m is located at a depth of 50 m and runs from the toe up to mid-slope region. Homogenous materials with variable properties are distributed within the model domain, which are called *stable rock mass*, *sliding zone* and *rockslide mass*. Depending on the allocation of these materials to the different model zones, large and small rockslides can be analyzed (Models B, C, D, E; compare Fig. 5). Like in the examples shown in Fig. 1, a region of *alluvial deposits* is located at the toe.

A mesh consisting of about 24,500 nodes was generated for the generic model in Seep/W, with a node density adjusted to the region size. For steady-state modeling the following boundary conditions are used: a fixed reservoir level at the toe of the slope (total head at an altitude of 1800 m), potential groundwater infiltration of 300 mm/a along the slope area from the crest (altitude of 2800 m) to the toe (altitude of 1800 m) and potential seepage face review at the whole slope. The bottom and right boundaries of the model were defined as no flow boundaries.

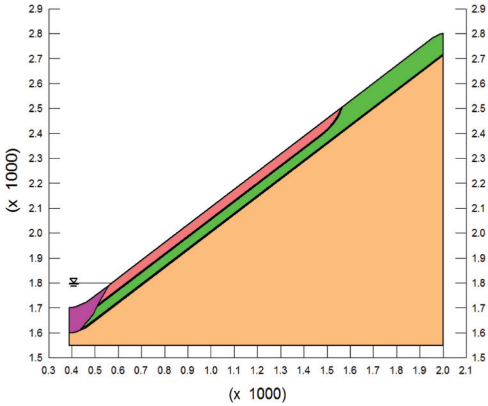

Fig. 2 - Geometric setup of the generic translational rockslide model. Scale is shown in meters

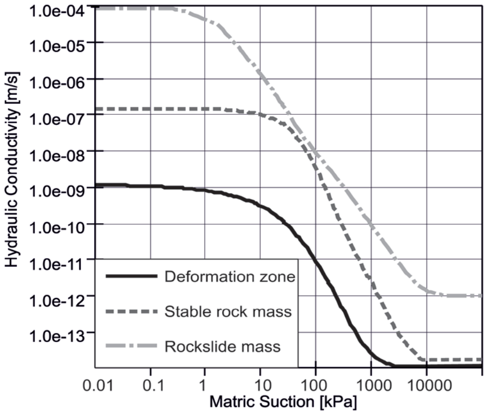

Fig. 3 - Hydraulic conductivity functions for different material types and base case parameter set

	Saturated Hydraulic Conductivity [m/s]			
	Stable Rock Mass	**Rockslide Mass**	**Sliding Zone**	**Alluvial Deposits**
Base Case	$1.5 \cdot 10^{-7}$	$8.9 \cdot 10^{-5}$	$1.2 \cdot 10^{-9}$	$1.0 \cdot 10^{-5}$
Parameter Var. 1	$1.5 \cdot 10^{-8}$	$8.9 \cdot 10^{-5}$	$1.2 \cdot 10^{-9}$	$1.0 \cdot 10^{-5}$
Parameter Var. 2	$1.5 \cdot 10^{-8}$	$8.9 \cdot 10^{-7}$	$1.2 \cdot 10^{-9}$	$1.0 \cdot 10^{-5}$
Parameter Var. 3	$4.5 \cdot 10^{-8}$	$8.9 \cdot 10^{-7}$	$1.2 \cdot 10^{-9}$	$1.0 \cdot 10^{-5}$

Tab. 1 - Saturated hydraulic conductivities applied for base case and parameter variations

If we consider the top of the model as a symmetric ridge and the left hand boundary as a symmetric lake, the right and left hand model boundaries have no boundary impacts on the modeling results. The impact of the lower model boundary should be minor, as hydraulic conductivity of stable rock masses tend to substantially decrease with depth below ground surface (e.g. Masset & Loew 2010).

ROCKSLIDE SATURATED/UNSATURATED HYDRAULIC CONDUCTIVITY

Fully saturated hydraulic conductivities were estimated based on parameter ranges as determined from the test sites described above. The base case saturated hydraulic conductivities are approximately 1E-4 m/s for the *rockslide mass* (Pisani *et alii,* 2010, Thoeny 2008), 1E-7 m/s for the *stable rock mass* (Woodbury & Smith 1987) and 1E-9 m/s for the *sliding zone* (Fischer *et alii,* 1998). Since the generic model also deals with groundwater flow and pressure in unsaturated parts of the slope, it is necessary to define hydraulic conductivity functions (characteristic curves) for the different rock masses. These functions describe how hydraulic conductivity is decreased in the unsaturated zone relative to groundwater flow in the fully saturated zone and how hydraulic conductivity is related to saturation, capillary pressure and pressure head.

In this study, fracture capillary pressure as a function of water saturation was estimated for the *stable rock mass* assuming a logarithmic normal distribution of fracture apertures (Pruess & Tsang 1990). A capillary pressure versus saturation function for the *sliding zones* was adopted from a laboratory test on a tectonic shear zone with cohesive fault gouge in granodioritic rock (Fischer *et alii,* 1998). For the *rockslide mass* similar characteristic curves were used, scaled to higher saturated hydraulic conductivity. Figure 3 illustrates these model input curves for the base case parameter set.

In this article, we also present results from a limited series of variations of hydraulic conductivity functions. For these parameter variations, saturated hydraulic conductivities were adapted to alternative conditions of the presented case studies and the corresponding hydraulic conductivity curves were shifted parallel to the base case curves of Fig. 3 (Tab. 1).

HYDRAULIC BEHAVIOR OF A GENERIC TRANSLATIONAL ROCKSLIDE MODEL

PORE PRESSURE DISTRIBUTIONS

Figure 4 illustrates the differences between fully saturated (Fig. 4a) and saturated/unsaturated (Fig. 4b) flow simulations in a homogeneous rock-slope with *stable rock mass* properties. The positions of the phreatic

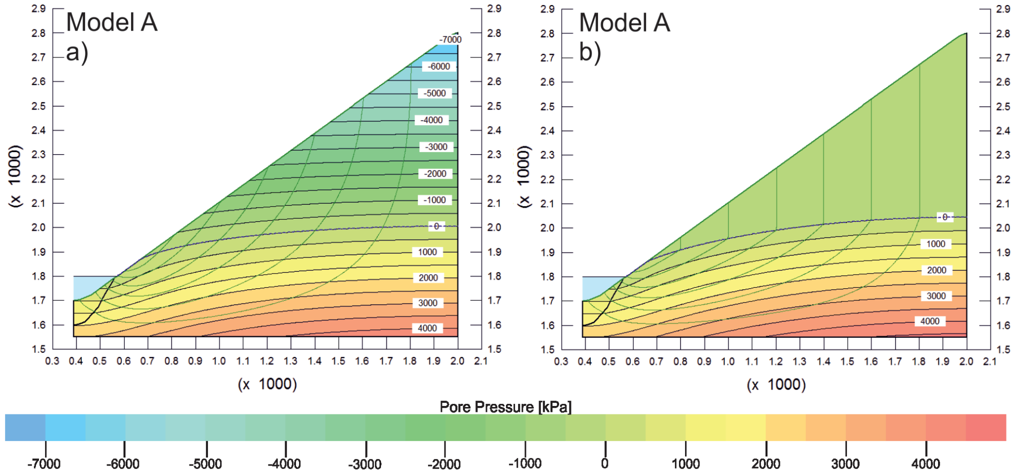

Fig. 4 - Groundwater flow lines, groundwater table (blue broken line) and pore pressures [kPa] for homogenous model A without rockslide, calculated for fully saturated (a) and saturated/unsaturated (b) conditions. Base case parameter set. Negative pore pressures in the fully saturated model (a) are meaningless

groundwater table, which is defined as zero pore pressure boundary at an assumed air pressure of zero, and the seepage face, which is the slope surface below the intersection with the groundwater table, have similar shapes but differ by about 500 kPa (50 m) below the mountain crest. The flow lines are slightly different in the saturated zones and substantially different in the unsaturated zones. The indicated negative pore pressures in the fully saturated model above the water table are meaningless. Therefore in this paper only results from saturated/unsaturated flow simulations are shown.

Variations in the flow field and pore pressure distributions of the different rockslide model types are illustrated in Figs 5 and 6. In all 4 model cases the groundwater table is deep as the ratio between infiltration (300 mm/a corresponding to 9.5E-9 m/s) and saturated rock mass hydraulic conductivity is much smaller than 1. Also, no significant seepage zone occurs above the lake level, and most of the groundwater discharge takes place at or below the lake level. In a rockslide that occupies about half of the slope (model B and C), most of the groundwater flow occurs at the base of the *rockslide mass*, independent of the existence or absence of a low-permeability sliding zone with clay gouge. This is due to the large contrasts in saturated and unsaturated hydraulic conductivities between the *rockslide mass* and the *stable rock mass*. In the saturated zone, a large pressure differential of about 350 kPa (35 m of water head) develops across the low permeability *sliding zone* in model C. The large rockslide occupying the entire slope (model D) leads to almost complete drainage and no groundwater recharge from precipitation into the deeper aquifer, showing a quasi-horizontal water table. Suction of up to 400 kPa develops around the *sliding zone*.

Groundwater table elevations for reduced *stable rock mass* and *rockslide mass* hydraulic conductivities are plotted in Figs 7 and 8. As shown in these figures, the saturated zones are very sensitive to hydraulic conductivity variations in the range of the groundwater recharge magnitude. For parameter variations 1 and 2 with a substantially reduced *stable rock mass* hydraulic conductivity, the water table is close to the crest of the mountain and generates substantial confined pore pressure conditions below the *sliding zone*. For parameter variation 3, with an intermediate saturated hydraulic conductivity of the *stable rock mass* the water table below the rockslide lies at an elevation of 2000 to 2100 m asl and again shows a perched aquifer above the *sliding zone* and with a deep unsaturated zone below in the upper part of the rockslide. A reduction in rockslide hydraulic conductivity (parameter variation 2 and 3) leads to a substantial increase in rockslide saturation and a seepage face extending about 50 m above the lake level (Figs 7 and 8).

PORE PRESSURE TRANSIENTS

Transient pore pressures resulting from temporarily variable groundwater recharge rates have been studied for rockslide model C and base case rock mass proper-

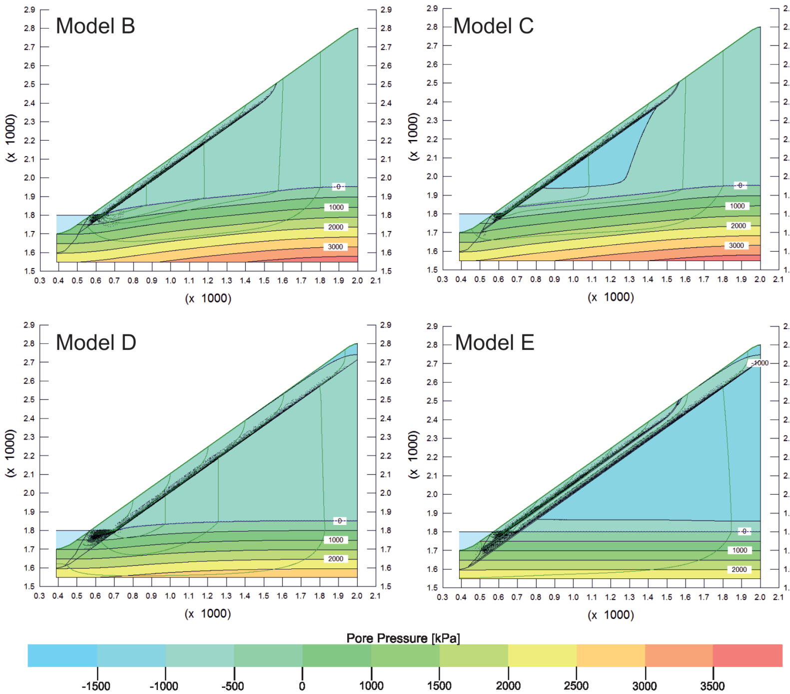

Fig. 5 - Modeled pore pressure distributions [kPa] and flow lines for landslide model B (small rockslide without sliding zone), model C (small rockslide with sliding zone), model D (large rockslide without sliding zone), and model E (large rockslide with a basal and an internal sliding zone). Base case parameter set

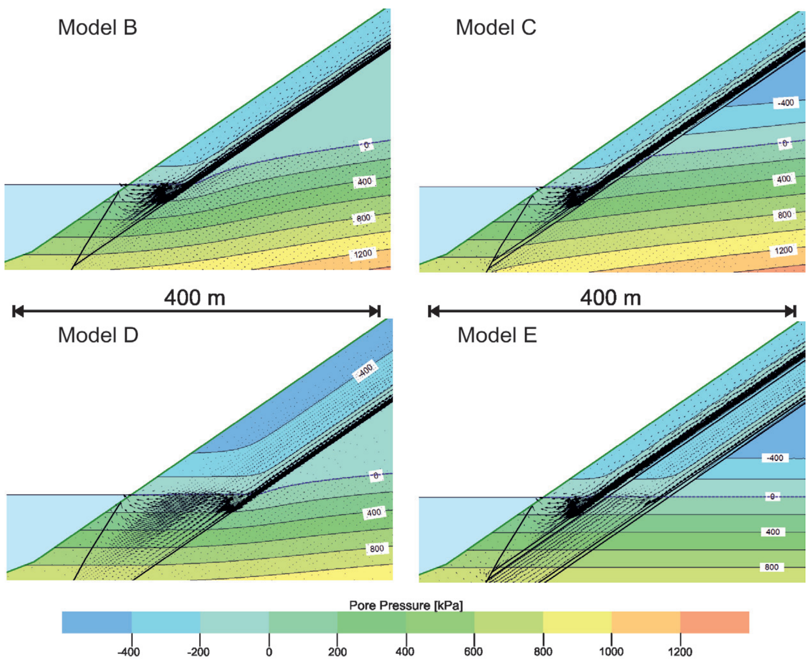

Fig. 6 - Modeled pore pressure distributions [kPa] and Darcy flow vectors for landslide model B (small rockslide without sliding zone), model C (small rockslide with sliding zone), model D (large rockslide without sliding zone), and model E (large rockslide with a basal and an internal sliding zone). Shown are details of Figure 5 at toe of model landslides

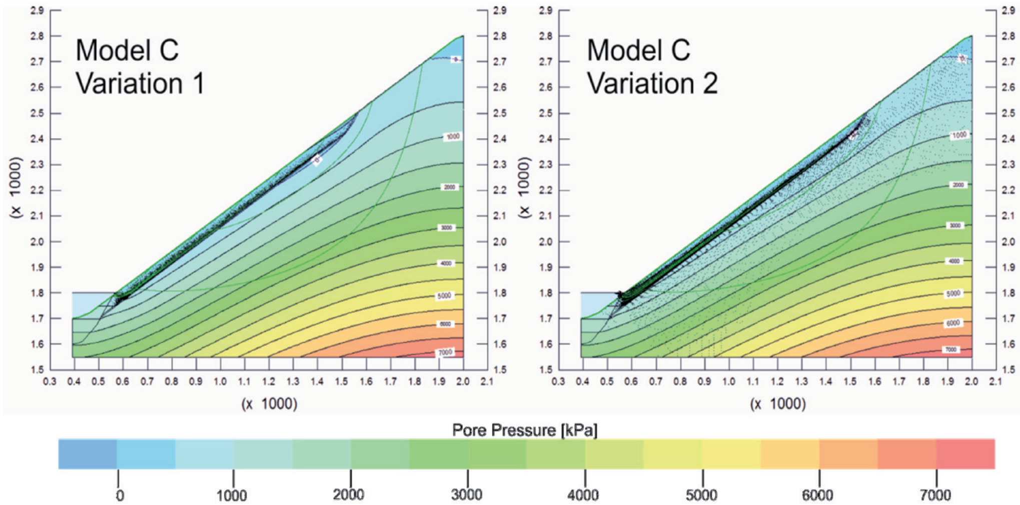

Fig. 7 - Parameter variations 1 and 2 for rockslide model C. Detailed legend see Fig. 5

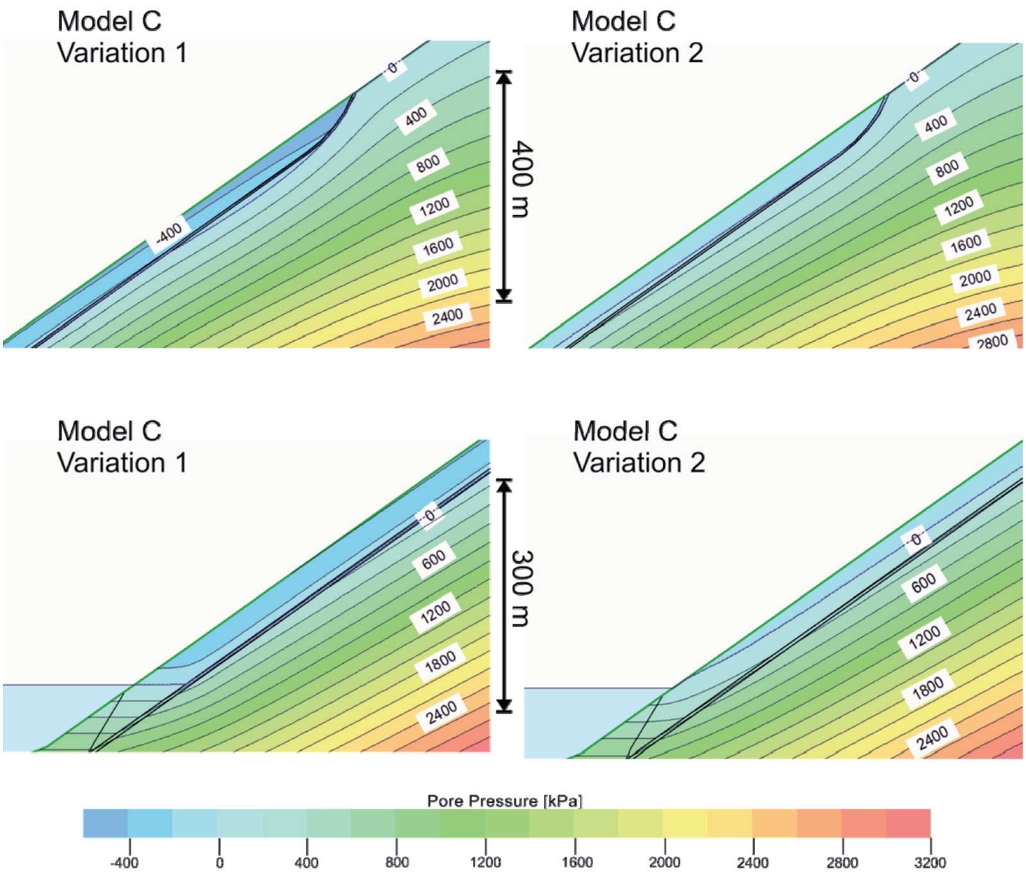

Fig. 8 - Parameter variations 1 and 2 for rockslide model C. Details of Fig. 7

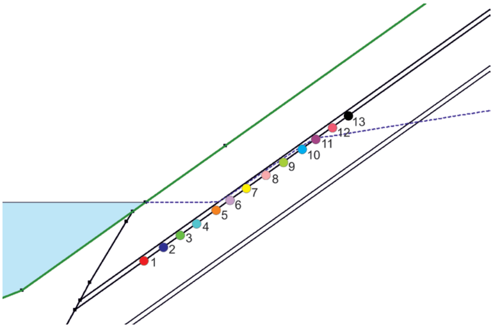

Fig. 9a

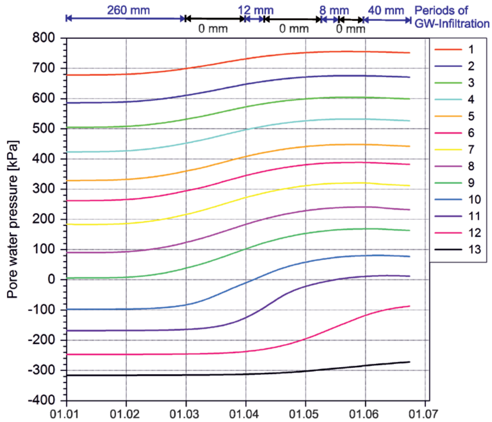

Fig. 9b

ties. These transients are modeled for strong groundwater recharge rates during snow melt in spring with an assumed duration of 30 days, a total recharge of 260 mm and moderate groundwater recharge events (12+8+40 mm) during 3 summer/fall rainstorms periods of about 1 week duration (e.g. Hansmann *et alii,* 2012). Figure 9 shows the resulting pore pressure transients along the lower boundary of the *sliding zone* in the toe region of the rockslide. For the assumed parameter values, saturated pore pressures below the groundwater table slowly respond to groundwater recharge from snow melt and reach peak values about 2.5 months after the end of the snow melt period. Also, negative pore pressures of up to 320 kPa (suction) above the groundwater table (monitoring points 10-13) decay in response to groundwater recharge from snow melt, but with a longer time shift. Summer rainstorms do not lead to any visible pore pressure changes in the landslide toe area.

DISCUSSION AND CONCLUSIONS

Even though the generic rockslide model presented above is very simple, and in many aspects far from reality, it can explain most of the key observations from the well-studied rockslides discussed in chapter 2. Pressure compartments bounded by low permeability fault gouge layers show the same order of magnitude pressure differentials as observed at Dutchman´s Ridge and Little Chief Slides. Major groundwater flows occur at the base of the *rockslide mass* and drain most of the slope recharge, as observed at the Aknes, Rosone and Dutchman´s Ridge rockslides. Below these high conductivity units deep, unsaturated zones might develop depending on the effective hydraulic conductivity of the *stable rock mass* below the rockslides.

Water table elevations within the *rockslide mass* strongly depend on saturated hydraulic conductivity, which varies by several orders of magnitude, depending on type and magnitude of gravitational and tectonic deformation. A high rockslide hydraulic conductivity of 1E-4 m/s leads to a narrow seepage face or one is completely situated below of the reservoir level, as in the case of Dutchman's Ridge and Little Chief Slide. A reduction of effective rockslide mass hydraulic conductivity to 1E-6 m/s leads to a substantial increase in saturation level and a seepage face reaching about 50 m in altitude. However, it is well-known that fractured crystalline rocks strongly show heterogeneous hydraulic conductivities at multiple scales (e.g. Masset & Loew 2010). Variable fracture aperture and connectivity distributions lead to equivalent rock mass hydraulic conductivity and flow porosity variations by many orders of magnitude and preferential groundwater flow paths with very high transmissivity. Therefore, the assumption of homogeneity and isotropy applied to the generic rockslide models is far from reality.

Variably saturated flow simulations are important to properly capture flow lines and pore pressure conditions. The characteristic curves for unsaturated flow and pressure in the *stable rock mass* and *sliding zone* are uncertain and will be critically investigated in future investigations. Especially the magnitudes of negative pore-water pressures in the unsaturated parts of the *stable rock mass* might be overestimated. For *rockslide masses* with a significant amount of total displacement (> several meters) the apertures of active fractures, i.e. fractures along which active displacements are observed, are typically significantly larger than the capillary pressure threshold of about

4 mm (WANG & NARASHIMHAN 1993). This implies that negative pore pressures are only expected to be significant in intact blocks of the *rockslide mass*. On the other hand seepage forces at the base of the highly fractured siding mass are an additional component affecting rockslide stability.

FREDLUND *et alii,* 1995 extend the classical slope stability limit-equilibrium relationships for homogeneous soils to unsaturated conditions. They show that in unsaturated soils two independent stress state variables define the shear strength τ: the effective angle of internal friction φ´ and the angle of the shear strength - matric suction relationship φ^b:

$$\tau = c' + (\sigma_n - u_a)\tan\varphi' + (u_a - u_w)\tan\varphi^b$$

where c´ is effective cohesion, σ_n is total normal stress on shear surface, u_a is pore-air pressure (often equal to atmospheric conditions) and u_w is pore-water pressure. Whereas the internal friction angle is assumed to be independent of suction, the φ^b value decreases with matric suction below the air entry pressure. At pore-water pressures above the air entry pressure both angles are equal. The shear-strength - soil suction relationship strongly depends on the saturation - matric suction relationship (VANAPALLI 1994). Fredlund *et alii,* 1995 show, that for steep soil slopes with critical slip surfaces located predominantly above the water table (base case parameter set), the safety factors significantly increase with suction and the critical slip surfaces move deeper into the slope. In the base case parameter set negative pore pressures of several 100 kPa develop in the *sliding zone* (model C and E, Figure 6) which are expected to have similar stabilizing effects.

ACKNOWLEDGEMENTS

The authors would like to thank the Tiroler Wasserkraft AG, ILF Consulting Engineers Ltd., GEO.ZT GmbH, and FFG (COMET) for supporting this work. We thank an anonymous reviewer for valuable comments, and Reto Thoeny, Lars Harald Blikra and Andrew Watson for field work, field visits and many fruitful discussions.

REFERENCES

BINET S. *et alii* (2007) - *In situ characterization of flows in a fractured unstable slope*. Geomorphology, **86**: 193-203.

BONZANIGO L., EBERHARDT E. & LOEW S. (2007) - *Long-term investigation of a deep-seated creeping landslide in crystalline rock. Part I. Geological and hydromechanical factors controlling the Campo Vallemaggia landslide*. Canadian Geotechnical Journal, **44**: 1157-1180.

CRAIG R.F. (2004) - *Craig's soil mechanics*. 7th Ed. Spon Press, 447 pp.

FISCHER U., KULLI B. & FLÜHLER H. (1998) - *Constitutive relationships and pore structure of undisturbed fracture zone samples with cohesionless fault gouge layers.* Water Resources Research, **34** (7): 1695-1701.

FREDLUND D.G. (1995) - *The stability of slopes with negative pore-water pressures*. Ian Boyd Donald Symposium on Modern Developments in Geomechanics, Monash University, Melbourne: 99-116.

FREI C. (2008) - *Groundwater flow at the Aknes Rockslide site (Norway), results of a multi-tracer test.* MSc Thesis Thesis, ETH Zurich, Zürich, 97 pp.

GANEROD G.V. *et alii* (2008) - *Geological model of the Aknes rockslide, western Norway.* Engineering Geology, **102**: 1-18.

GEO-SLOPE INTERNATIONAL LTD (2008) - *Seepage modelling with SEEP/W 2007 - An Engineering Methodology.* 3rd Ed. Canada, 305 pp.

GRONENG G., CHRISTIANSEN H.H., NILSEN B. & BLIKRA L.H. (2011) - *Meteorological effects on seasonal displacements of the Aknes rockslide, western Norway.* Landslides, **8**: 1-5.

HANSMANN J. (2012) - *Analysis of transient surface deformations above the Gotthard Base Tunnel (Switzerland)*. Unpublished Dissertation ETH Zürich: **20177**, 180 pp.

HUNGR O., COROMINAS J. & EBERHARDT E. (2005) - *Estimating landslide motion mechanisms, travel distance and velocity.* In: HUNGR O., FELL, COUTURE & EBERHARDT (EDS). *Landslide risk management.* Proc. of an Int. Conference, Vancouver. Taylor and Francis Group, London.

IMRIE A.S., MOORE D.P. & ENEGREN E.G. (1991) - *Performance and maintenance of the drainage sytem at Downie Slide.* In: BELL (ED.). International Symposium on Landslides. ISL IV. Balkema, Christchurch. 751-757.

KALENCHUK K.S., HUTCHINSON D.J., DIEDERICHS M. & MOORE I. (2012) - *Downie Slide, British Columbia, Canada.* In: CLAGUE J.J. & STEAD D. (ED.). *Landslide: types, mechanisms and modeling*. Cambridge University Press: 345-358.

LOEW S., GISCHIG V., MOORE D.P. & KELLER-SIGNER A. (2012) - *Monitoring of potentially catastrophic rockslides*. In: EBERHARDT *et alii* (ED.) - *Landslides and engineered slopes: protecting society through improved understanding.* International Symposium on Landslides ISL Banff. Taylor and Francis Group: 101-116.

MASSET O. & LOEW S. (2010) - *Hydraulic conductivity distribution of crystalline rocks, derived from inflows to tunnels and gelleries in the Central Alps, Switzerland*. Hydrogeology Journal, **18**: 863-891.

MOORE D.P. (1992) - *Panelist Contribution: Stabilization of Downie Slide and Dutchman´s Ridge*, International Conference on Soil Mechanics and Foundation Enginering. ICSMFE Conference XII. Balkema, Rio de Janeiro. 3063-3065.

MOORE D.P. & IMRIE A.S. (1995) - *Stabilization of Dutchman´s Ridge*. In: BELL (ED.), International Symposium on Landslides. ISL VI. Balkema, Christchurch, pp. 1783-1788.

MUALEM Y. (1976) - *A new model for predicting the hydraulic conductivity of unsaturated porous media*. Water Resources Research, **12**: 513-522.

PISANI G., CASTELLI M. & SCAVIA C. (2010) - *Hydrogeological model and hydraulic behaviour of a large landslide in the Italian Western Alps.* Nat. Hazards Earth Syst. Sci., **10**: 2391-2406

PRUESS K. & TSANG Y.W. (1990) - *On two-phase relative Permeability and Capillary Pressure of Rough-Walled Rock Fractures*. Water Resources Research, 26, No. **9**: 1915-1926.

SCHEIDEGGER A.E. (1974) - *The physics of flow through porous media*. 3rd Edition, University of Toronto Press, 353 pp.

SIDLE R.C. & OCHIAI H. (2006) - *Landslides: processes, prediction, and land use*. Water Resources Monograph, 18. AGU, Washington.

THOENY R. (2008) - *Dynamic fluid electrical conductivity logging for identification and characterization of preferential groundwater flow in the Aknes rockslide (Norway).* MSc Thesis Thesis, ETH Zurich, Zürich, 105 pp.

VAN GENUCHTEN M.TH. (1980) - *A closed-form equation for predicting the hydraulic conductivity of unsaturated soils.* Soil Science Society of America Journal, **44**: 892-898.

VANAPALLI S.K. (1994) - *Simple test procedures and their interpretation in evaluating the shear strength of an unsaturated soil.* Ph.D. Thesis, University of Saskatchewan, Saskatoon, SK, Canada.

WANG J.S.Y. & NARASIMHAN T.N. (1985) - *Hydrologic mechanisms governing fluid flow in a partially saturated, fractured, porous medium.* Water Resources Research, **21** (12): 1861-1874.

WANG J.S.Y. & NARASIMHAN T.N. (1993) - *Unsaturated Flow in Fractured Porous Media*. In: BEAR J., TSANG C.F. & DE MARSILY G. (EDS). *Flow and Contaminant Transport in Fractured Rock*. Academic Press, 560 pp.

WATSON A.D., MOORE D.P., STEWART T.W. & PSUTKA J.F. (2007) - *Investigations and monitoring of rock slopes at Checkerboard Creek and Little Chief Slide*. In: EBERHARDT E., STEAD D. & MORRISON (EDS.). *Rock mechanics: meeting society´s challanges and demands.* Taylor & Francis Group, Vancouver, 1015-1022.

WOODBURY A.D., SMITH L. & DUNBAR W.S. (1987) - *Simultaneous inversion of hydrogeologic and thermal data 1. Theory and application using hydraulic head data.* Water Resources Research, **23** (8): 1586-1606.

ZANGERL C., EBERHARDT E. & PERZLMAIER S. (2010) - *Kinematic behaviour and velocity characteristics of a complex deep-seated crystalline rockslide system in relation to its interaction with a dam reservoir*. Engineering Geology, **112** (1-4): 53-67

